Computer Vision - CVWW'04
Proceedings of the 9th Computer Vision Winter Workshop,
Piran, Slovenia, 4-6 February 2004, pp. 31-40

3D Puzzling of Archaeological Fragments *

Martin Kampel and Robert Sablatnig
Vienna University of Technology
Institute of Computer Aided Automation
Pattern Recognition and Image Processing Group
Favoritenstr.9/183-2, A-1040 Vienna, Austria
{kampel,sab}@prip.tuwien.ac.at

Abstract

A major obstacle to the wider use of 3D object reconstruction and modeling is the extent of manual intervention needed to construct 3D models. Such interventions are currently massive and exist throughout every phase of a 3D reconstruction project: collection of images, image management, establishment of sensor position and image orientation, extracting the geometric detail describing an object, merging geometric, texture and semantic data. This work aims to develop a solution for automated documentation of archaeological pottery, which also leads to a more complete 3D model out of multiple fragments. Generally the 3D reconstruction of arbitrary objects from their fragments can be regarded as a 3D puzzle. In order to solve it we identified the following main tasks: 3D data acquisition, orientation of the object, classification of the object and reconstruction.We demonstrate the method and give results on synthetic and real data.

1 Introduction

Reassembly of fragmented objects from a collection of thousands randomly mixed fragments is a problem that arises in several applied disciplines, such as archaeology, failure analysis, paleontology, art conservation, and so on. Solving such jigsaw puzzles by hand may require years of tedious and delicate work, consequently the need for computer aided methods is obvious [9]. The assembling of an object from pieces is called mosaicing [7]. It is similar to the automatic assembly of jigsaw puzzles, which among others has been addressed by [1]. In [6] a system for analyzing and assembling a 2D image of pieces of a jigsaw puzzle is presented. The matching method is based on the shape and color characteristics of the pieces. However these approaches rely on specific characteristics of the pieces like color, critical points, or no gaps between matching pieces.

*This work was partly supported by the Austrian Science Foundation (FWF) under grant P13385-INF, the European Union under grant IST-1999-20273 and the Austrian Federal Ministry of Education, Science and Culture.

In archaeology, most of the finds are in form of fragments especially in the area of ceramics. Therefore mosaicing is of great interest in this field since it enables both, a real and a virtual reconstruction of the original object. Most of the ceramic is rotationally symmetric and using this fact, one can solve the mosaicing problem even if there are gaps between the fragments, just like a human would solve the problem. We work with fragments of rotational symmetric pottery. Figure 1a shows a box filled with archaeological fragments, which possibly could fit to each other. Figure 1b illustrates manually identified, matching fragments.

(a) (b)

Figure 1: Archaeological objects: (a) Box with possibly, matching fragments, (b) Matching fragments.

More generally mosaicing can be seen as a special case of object recognition by approximate outline matching: The specific problem of identifying adjacent ceramic fragments by matching the shapes of their outlines was considered by Üçoluk and Toroslu [17]. They represent the 3D fragments by their boundary curves. From the 3D boundary curve data, curvature and torsion scalars are computed. A noise tolerant matching algorithm serves to find the best match of two such circular strings. Hori et. al. [2] propose a method for joint detection among two potsherds designed for pottery fragment outlines. They consider that 2D images instead of 3D shape data are applicable. Their approach is based on a partial verification method of a pair of contours without knowledge of the shape features of a piece. Kong et. al. [5] approach the jigsaw problem in two stages: first, local shape matching aims to find likely candidate pairs for adjacent fragments. Second ambiguities resulting from local shape matching are resolved by a global solution. The matching is based on the notion of an alignment curve to represent a correspondence between two curves. 2D Potsherd reconstruction based on shape similarities is presented by Kanoh et. al. [4]. In a first step they join potsherds in two dimensions. The contour of a potsherd is divided into sub-contours by salient points [14], and the matching of the sub-contours is performed by P-type Fourier descriptors. In the second phase, three dimensional shape is recovered by mapping the 2D points into the 3D coordinate system of a cone or a cylinder. Marques et al. [10] present a 2D object matching technique based on the comparison of a reference contour to the contours in the image partition. The comparison is based on a distance map that measures the Euclidean distance between any point in the image

to the partition contours.

H.C.G. Leitão introduced a method for automatic reassembly of two-dimensional fragments [8]. Together with Stolfi [9] she demonstrates a multiscale matching method based on the idea that the outlines of two matching fragments are two noisy copies of the same time-domain signal. They compute the curvature encoded fragment outlines in order to compare possible matching candidates. To reduce the cost of computing the optimum pairing for a candidate, they progressively increase scales of resolution. The implementation is restricted to flat objects, such as tiles and murals. For curved fragments the three-dimensional geometry of the fracture line must be recovered with fairly high resolution, so as to have a representation of the fracture line that is insensitive to the fragment's orientation in three dimensions. G. Papaioannou et. al. [11, 13] present a semi-automatic reconstruction of archaeological finds from a geometric point of view: they rely on the broken surface morphology to determine correct matches between fragments. In the first stage they estimate coarse surface regions (i.e. the fractured side of the fragment) by surface bumpiness estimation [12]. In the second stage, a matching error is calculated for all candidate regions of every possible pair of fragments.

Summarizing existing techniques on the assemblage of virtual pots we observe a main focus on the analysis of the outline of the break curve: 2D outline matching is most common [9, 4, 5, 1, 6], but work on 3D outline matching exist [17]. Surface matching of fractured surfaces is proposed in [11]. So far, no complete system from acquisition to reconstruction has been described.

This paper focuses on the reconstruction of pottery out of many fragments. With respect to our previous work [16], the paper describes the finding and matching of candidate fragments as its main contribution.

Our approach to pottery reconstruction is based on the following main tasks: After acquiring 3d data with the Minolta VIVID 900, we start with the estimation of the correct orientation of the fragment, which leads to the exact position of a fragment on the original vessel. Next, the classification of the fragment based on its profile section provides a systematic view of the material found and allows us to decide to which class an object belongs presented in Section 2. Since we know the orientation of the candidate fragments we defined a two-degrees-of-freedom search space for representing the alignment of two fragments. A matching algorithm based on the point-by-point distance between facing outlines is proposed in Section 3. Reconstruction results on synthetic and real data are given in in 4, followed by conclusions and outlook on future work.

2 Determination of matching candidates

In order to find matching candidates the fragments are classified based on absolute measurements (e.g. diameter, height, ...) and the segmentation of the profile line into so called characteristic points. The classification leads to primitives and attributes describing the fragments unambiguously [3]. In order to find the confidence between two fragments, a description language is applied. A vessel or fragment is transformed into the description language by using the primitives and attributes found. In order to find the candidate fragments that could match

a fragment the generated description is compared with already existing descriptions. Comparison of newly found fragments of unknown type is performed by comparing the description of the new fragment with the description of already classified fragments. The fragment structure is formed by its *shape features* (or geometric features like the profile) and its *properties* (or material like clay, color and surface). The description of the fragment is structured in a description language consisting of primitives and relations. Primitives are a representation of shape features, relations represent the properties.

The description language, which was originally designed to solve 2D automatic visual inspection problems [15], is applied and extended in order to solve the classification problems. The actual profile contains features, which are a representation of shape features. To accomplish classification, primitives are further subdivided into part-models (or part- primitives), the consistency between part-primitives is established by relations among part parameters.

Formally, the description language is a graph $G =< O, R >$, where $O = \{m|1 <= m <= n\}$ denotes the set of nodes and $R = \{< c, d > |c, d \in O\}$ the set of arcs. A node O consists of different sub-objects or primitives. Each node has different attributes a, with weights w, and a tolerance $T(a)$ defined as

$$T(a) = \begin{cases} 1, \text{if} |a^{db} - a^{nw}| \leq c, \text{ and} \\ \frac{1}{|a^{db} - a^{nw}|} \text{ otherwise} \end{cases} \quad (1)$$

where c is the allowed tolerance, a^{db} denotes the value of attribute a in the archive, and a^{nw} the value of the attribute a of the object.

Two nodes are in relation according to R. Each relation $< c, d >$ is decomposed into k sub-relations between the same nodes, each with a weight v and a tolerance $T(r)$. The shape primitive $S1$ is subdivided into c different shape primitives (such as profile, diameter and the like). For each of these shape primitives n different sub-primitives (such as rim, wall and the like) are defined. Since the manual segmentation of the profile varies, tolerances and weights are included in the description.

The weights w and v are necessary for classification. Each property has a certain weight in order to verify the corresponding description to a given fragment. The verification of fragment to description consists of verifying whether the number and type of features and primitives are the same. Next, attributes and relations are checked to verify whether they match within given tolerances. Comparing all attributes of a node and its successors with the model carries out the verification process. The confidence for a node can be computed based on the result of the comparison:

$$conf(p) = \sum_{g=1}^{n} w_g * T(a_g) + \sum_{(p,g)}^{m} v_{(p,q)} * conf(q). \quad (2)$$

where w_g are the weights of the attributes of the nodes and $v_{(p,q)}$ the weights of the sub-relations of the arcs. Observe that n, the number of attribute values, and m, the number of arcs, depend

on the node p. Moreover, for leaves we have:

$$conf(p) = \sum_{g=1}^{n} w_g * T(a_g). \tag{3}$$

This enables us to compute the confidence of a node by summing up the weighted tolerances of each attribute of the node and the overall confidence of the subgraph connected to this node. By computing the consistency for different descriptions, the one with the highest confidence value can be chosen if the confidence is above a certain threshold. For a given profile all primitives are represented in the description of the profile.

3 Fragment Matching

The optimal pairing of matching candidates obtained serves as input for the fragment matching part. Consequently we know those pairs of fragments which were probably adjacent in the original object. We virtually glue two matching fragments together by computing the transformation parameters, which bring two candidate fragments into alignment.

In order to represent the matching of two fragments, G. Papaioannou et. al. [11] describe seven pose parameters. In their approach the two fragments are first prealigned so that their broken facets face each other. In our case we know the orientation of a fragment, consequently we prealign two candidate fragments by simply aligning their axis of rotation. As a result, a two-degrees-of-freedom continous search space is defined. The transformation which matches two candidate fragments consists of a translation along the z-axis with parameter T_z and a rotation around the z-axis with parameter R_z (see Figure 2a).

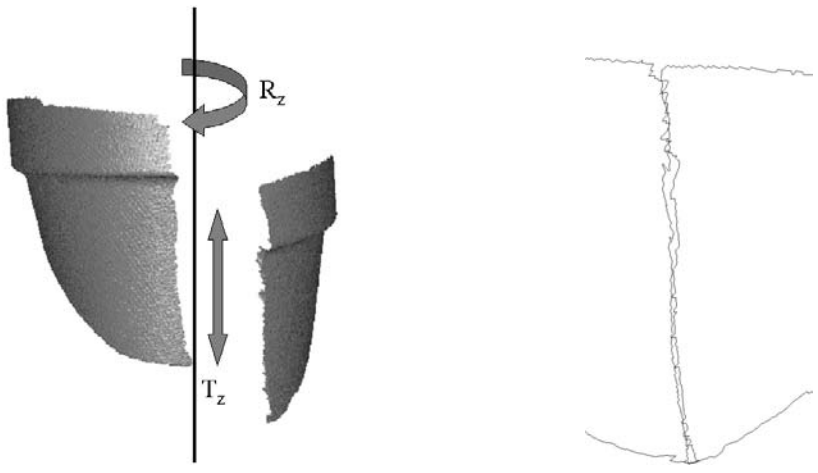

(a) (b)

Figure 2: (a) Fragment Matching with 2-degrees-of-freedom (b) Matching outlines.

The basic concept in our method for estimating R_z is that the best fit is likely to occur at the relative pose which minimizes the point-by-point distance between the facing outlines. For

this reason, we introduce a matching error ϵ_M based on the mean Euclidian distance between the corresponding points of the outlines of the candidate fragments with points $X = (x, y)$ and $X' = (x', y')$:

$$\epsilon_M = \frac{1}{N} \sum_{i=1}^{N} \sqrt{(x_i - x'_i)^2 + (y_i - y'_i)^2}. \quad (4)$$

where N is the number of data points used. The height of the fragment limits the length of the matching segments. Different fragments types lead to the following matching possibilities:

A Rim fragments: first T_z is computed by aligning the rim along the orifice plane [3]. Next R_z is estimated, so that the positioning transformation with the smallest matching error ϵ_M is considered to be the correct position. Figure 2b shows matching outlines of two rim-fragments.

B Bottom fragments: first T_z is computed by aligning the bottom along the base plane. Next R_z is estimated in the same way as for rim fragments.

C Wall fragments: Candidates are first aligned along their profile sections. Next R_z is estimated in the same way as for rim fragments. Since it is not clear whether a new candidate fragment is in bottom up or bottom down position, we have to compute R_z and T_z for both positions. The positioning transformation with the smallest matching error ϵ_M is considered to be the correct position.

Matching algorithm

1. Define reference fragment F_{ref} with its axis of rotation ROT_{ref}: defines a new pot P, creates the pot coordinate system, ROT_{ref} is aligned to the z-axis.

2. Prealignment of the candidate fragment F_{cand} by its axis of rotation ROT_{cand}: ROT_{cand} is aligned to ROT_{ref}. This results in a two-degrees-of-freedom search space.

   (a) translation T_z along the axis of rotation (up/down).

   (b) rotation R_z around the axis of rotation.

3. Estimation of the translation parameter T_z: search for minimal distance d between all y-values (radius) of the profile of F_{ref} and the profile of F_{cand}.
   Exception A: Rim fragments are aligned along the orifice plane.
   Exception B: Bottom fragments are aligned along the base plane.

   When the candidate fragment is a wall fragment, the minimal distance d is computed for both positions, and the one with the smaller is considered to be the correct position.

4. Estimation of the rotation parameter R_z by finding the position with the smallest matching error ϵ_M.

4 Results

In order to evaluate the results we have tested our method on synthetic 3D data of three parts of a synthetic pot. The orientation of the fragments is defined, which leads to three perfect matching parts. The experiment has shown a 100% theoretical accuracy of the approach. To find out if the method is working on real data, we used a flowerpot with known dimension. We broke this flowerpot into 5 parts (see Figure 3) in order to get data of matching fragments of a whole pot. We got three rim fragments, one wall fragment and one bottom fragment. Each part was digitized leading to a front and back view of each fragment. The biggest part (nr. 2) covers half of the pot and consists of 135070 triangles, whereas the smallest consists of 8210 triangles.

Figure 3: 5 parts of a flowerpot.

Next we computed the orientation of the fragments, which leads to four matching candidates and one not processable object: a large part of the bottom fragment (Part 4) consists of flat area. It was therefore excluded from further processing due to its curvature being too low.

Starting with part one as reference fragment for each candidate a matching error was computed. Next part two was defined as reference fragment and again for each remaining candidate a matching error was computed. This procedure was continued until no candidate remained. Table 1 summarizes T_z, R_z and the matching errors for each possible candidate. $RF_{nr.}$ and $CF_{nr.}$ denote the number of the reference fragment and the number of candidate fragment respectively, and ϵ_M denotes the matching error. The value of ϵ_M for correct matches ranges from 1.12 to 0.63, the combination of part 3 and 5 shows an incorrect match with an error ϵ_M of 12.92.

Figure 4a displays the resulting match of part 1 and part 3 as both parts are rim fragments. Figure 4b shows the resulting match of part 1 and part 5. Since part 5 is a wall fragment the ϵ_M was computed for both possible positions, and the position with lower ϵ_M was finally choosen. Figure 4c shows the final reconstruction of the pot. Correct matches for all four candidate fragments have been found. The missing bottom of the pot is due to part 4, not being processable because of its flat shape.

We applied our technique to real archaeological fragments (Nr: 319-71, 209-71 from the late Roman burnished ware of Carnuntum [16], as shown in Figure 5a and b. Both pieces are rim fragments. Each part was digitized leading to a front and back view of each fragment.

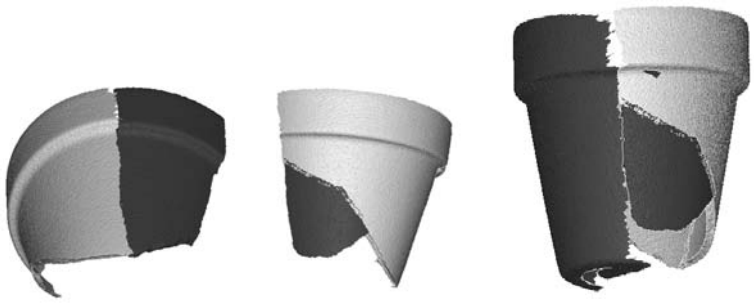

(a) (b) (c)

Figure 4: Matched parts: (a) part 1 and part 3 (b) part 1 and part 5 (c) Matching parts 1, 2, 3, and 5.

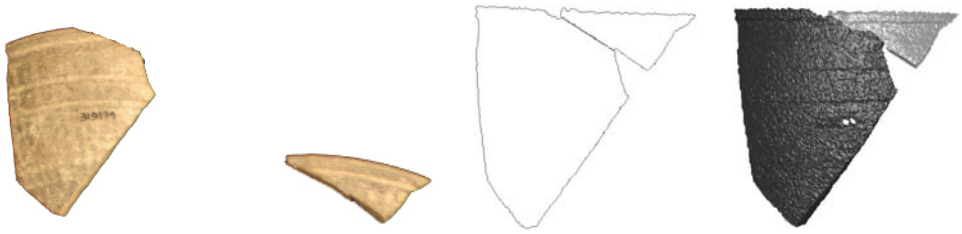

(a) (b) (c) (d)

Figure 5: Archaeological rim fragments: (a) Part1, (b) Part 2, (c) Matching outlines, (d) Matching parts.

Next we computed the orientation of the fragments. The alignment along the orifice plane allowed the estimation of $T_z = 7.49$cm. The smallest $\epsilon_M = 0.31$ was found for $R_z = 3.35°$. Figure 5c shows the matched outlines of the two fragments and Figure 5d shows the final reconstruction. Due to the dense sampling and the non eroded fracture sides of the original fragments (the fragment was possibly broken during excavation) the reconstruction method managed to yield to a small matching error.

Another example on real archaeological fragments was done on the common ware of Sagalassos [16]. One rim and two wall fragments were recorded and processed. The number of points and triangles of the front and back views ranges from 9000 to 16500 triangles. After the estimation of the orientation we started with part one as reference fragment and computed for each candidate a matching error. Next part two was defined as reference fragment and again for each remaining candidate a matching error was computed. This procedure was continued until no candidate remained. Table 1 summarizes T_z, R_z and the matching errors for each possible candidate. Correct matches were found between part one and part two ($\epsilon_M = 1.32$) and part two and part three ($\epsilon_M = 1.21$). No correct match was found between part one and part three ($\epsilon_M = 14.81$), because there was no alignement of the profile sections (part one is on top of part three). Nevertheless all three fragments were matched together, since the matching of part two suceeded for both candidates.

The results demonstrate the possibility of automatically matching adjacent fragments by

Ware	$RF_{nr.}$	$CF_{nr.}$	T_z [mm]	R_z [deg]	ϵ_M
Flowerpot	1	2	12.03	22.81	1.12
Flowerpot	1	3	8.67	-41.29	0.81
Flowerpot	1	5	9.34	73.21	0.63
Flowerpot	2	3	-4.94	17.61	0.92
Flowerpot	2	5	-10.02	-26.75	0.71
Flowerpot	3	5	11.10	32.99	12.92
Carnuntum	1	2	7.49	3.35	0.31
Sagalassos	1	2	-4.29	11.70	1.32
Sagalassos	1	3	-1.61	7.59	14.81
Sagalassos	2	3	-5.19	15.76	1.21

Table 1: Results of the matching process.

our method. It works for fragments which can be orientated and classified by our approach with one exception: two adjacent fragments on top of each other cannot be matched by our method, because they do not have overlapping profile sections. Furthermore if the surface of the fragment is too flat or too small (that would lead to an incorrect axis of rotation) or the classification is not known, the fragment is not considered for reconstruction automatically.

5 Conclusion

We have proposed a method for the assembly of an object from pieces, which in our case means the reconstruction of an archaeological pot from its fragments. The outcome on vessel reconstruction out of multiple fragments was described by real 3D data. The ceramic documentation and reconstruction system described was recently integrated into the virtual excavation reconstruction project 3D MURALE. Future work will be directed towards setting up a pottery database with more then 100 fragments and applying the algorithm to find matching pieces.

References

[1] G. C. Burdea and H. J. Wolfson. Solving Jigsaw Puzzles by a Robot. *IEEE Transactions on Robotics and Automation*, 5(5):752–764, 1989.

[2] K. Hori, M. Imai, and T. Ogasawara. Joint Detection for Potsherds of Broken Earthenware. In *IEEE Computer Society Conference on Computer Vision and Pattern Recognition (CVPR '99)*, volume 2, pages 440–445, June 1999.

[3] M. Kampel. *3D Mosaicing of Fractured Surfaces*. PhD thesis, TU-Vienna, Inst. f. Automation, Pattern Recognition and Image Processing Group, 2003.

[4] M. Kanoh1, S. Kato, and H. Itoh. Earthenware reconstruction based on the shape similarity among potsherds. *Society for Science on Form*, 16(1):77–90, 2001.

[5] W. Kong and B.B. Kimia. On solving 2D and 3D puzzles using curve matching. In *IEEE Computer Society Conference on Computer Vision and Pattern Recognition (CVPR '01)*, volume 2, pages 583–590, 2001.

[6] D.A. Kosiba, P. M. Devaux, S. Balasubramanian, T.L. Gandhi, and R. Kasturi. An Automatic Jigsaw Puzzle Solver. In *Proc. of the 12th IAPR International Conference on Pattern Recognition, Jerusalem*, volume 1, pages 616–618. IEEE-Computer Society Press, 1994.

[7] Langenscheidt. *Langenscheidts Fremdwörterbuch*. Friedhelm Hübner, 1989.

[8] H. C. G. Leitão. *Reconstrução Automática de Objetos Fragmentados*. PhD thesis, Inst. of Computing, Univ. of Campinas, 1999.

[9] H. C. G. Leitão and J. Stolfi. A Multiscale Method for the Reassembly of Two-Dimensional Fragmented Objects. *IEEE Trans. on Pattern Analysis and Machine Intelligence*, 24(9):1239–1251, 2002.

[10] F. Marques, , M. Pardis, and R. Morros. Object matching based on partition information. In *IEEE Computer Society International Conference on Image Processing*, volume 2, pages 829–832, 2002.

[11] G. Papaioannou, E.A. Karabassi, and T. Theoharis. Virtual archaeologist: Assembling the past. *IEEE Computer Graphics*, 21(2):53–59, March-April 2001.

[12] G. Papaioannou, E.A. Karabassi, and T. Theoharis. Segmentation and Surface Characterization of Arbitrary 3D Meshes for Object Reconstruction and Recognition. In *IEEE Int. Conference on Pattern Recognition*, pages 734–737, September Barcelona, 2000.

[13] G. Papaioannou, E.A. Karabassi, and T. Theoharis. Automatic Reconstruction of Archaeological Finds- a Graphics Approach. In *Proc. 4th Intern. Conf. in Computer Graphics and Artificial Intelligence*, pages 117–125, May Limoges, 2000.

[14] A. Rosenfeld and E. Johnston. Angle detection on digital curves. *IEEE Transactions on Computers*, 22:875–878, 1973.

[15] R. Sablatnig. *A Highly Adaptable Concept for Visual Inspection*. PhD thesis, TU-Vienna, Inst. f. Automation, Pattern Recognition and Image Processing Group, 1997.

[16] R. Sablatnig and M. Kampel. Model-based registration of front- and backviews. *Computer Vision and Image Understanding*, 87(1):90–103, 2002.

[17] G. Üçoluk and H. Toroslu. Automatic Reconstruction of Broken 3D surface objects. *Computers and Graphics*, 23(4):573–582, 1999.